

# Doping with a special carbohydrate, C<sub>9</sub>H<sub>11</sub>NO, to improve the $J_c$ - $B$ properties of MgB<sub>2</sub> tapes

X. P. Zhang<sup>A</sup>, D. L. Wang<sup>A</sup>, Z. S. Gao<sup>A</sup>, L. Wang<sup>A</sup>, Y. P. Qi<sup>A</sup>, Z. Y. Zhang<sup>A</sup>, Y. W. Ma<sup>A</sup>, S. Awaji<sup>B</sup>, G. Nishijima<sup>B</sup>, K. Watanabe<sup>B</sup>

<sup>A</sup> Institute of Electrical Engineering, Chinese Academy of Sciences, Beijing 100190, China

<sup>B</sup> Institute for Materials Research, Tohoku University, Sendai 980-8777, Japan

## 1. Introduction

MgB<sub>2</sub> has been hotly studied since its superconductivity was observed [1]. It was thought as a potential engineering material because of the high transition temperature  $T_c$ , low material cost, simple fabrication process, and reasonable upper critical field  $H_{c2}$  values. One promising application of MgB<sub>2</sub> superconductor is in the magnetic resonance imaging (MRI) magnet that can work around 20 K, a temperature range that can be readily reached by a cryogen-free cryocooler [2]. For this reason, a huge amount of work has been carried out to improve the current carrying capability of MgB<sub>2</sub> wires/tapes, so that they can be used to construct MRI magnets.

It has been shown that the critical current density  $J_c$  of MgB<sub>2</sub> is a complex balance between connectivity,  $H_{c2}$ , and flux pinning [3]. As proved by many groups,  $H_{c2}$  can be increased rather easily by disorder introduction, chemical doping, or neutron irradiation. And the flux pinning ability in high magnetic field can be enhanced by artificially made flux pinning centers, such as defects and precipitates [4]. For the grain connectivity improvement, the usually used method is to increase the core density [5] or to enhance the grain linkages by chemical doping. Accordingly, chemical doping has been widely used to improve the  $J_c$  of MgB<sub>2</sub> materials. A lot of dopants have been tried in the past years. In them, carbohydrates as promising dopants to MgB<sub>2</sub> were specially investigated recently. Carbohydrate materials can provide elemental carbon, which is much favorable for the C substitution for B and can obviously improve  $H_{c2}$ , when they are

heated above their decomposition temperature. On the other hand, compared with other nano-carbon doping method, using carbohydrate can be more attractive since highly uniform mixing is possible.

The doping effect of carbohydrates to MgB<sub>2</sub> has remarkable difference because of their different physical/chemical properties. As a good dopant, the carbohydrate should not contain too much oxygen element in order to avoid the impairment of MgO to grain linkages [6]. On the other hand, it should have appropriate melting point and decomposition temperature. A suitable melting point means that the carbohydrates can be homogeneously distributed in the raw powders before chemical reaction happens, getting a uniform dispersion in superconducting core. Furthermore, an appropriate decomposition temperature will be helpful to get reactive carbon atoms during the formation of MgB<sub>2</sub> crystals. We found that commercial 4-dimethylaminobenzaldehyde, C<sub>9</sub>H<sub>11</sub>NO, can meet all of the above point, since it has a low melting point (73-75°C) and slightly oxygen element content (4.5at.%).

In this paper, we report that a significant in-field  $J_c$  enhancement in MgB<sub>2</sub> tapes can be easily achieved by doping with C<sub>9</sub>H<sub>11</sub>NO, which has several favorite features as MgB<sub>2</sub> dopant. The effects of sintering temperature on the crystallization,  $T_c$ ,  $H_{c2}$ , and the magnetic field dependence of  $J_c$  have been investigated in detail.

## 2. Experimental

MgB<sub>2</sub> tapes were prepared by the *in situ* powder-in-tube (PIT) method. Commercial powders of magnesium (-325 mesh, 99.8%), boron (amorphous, 2-5 μm, 99.99%) and 4-dimethylaminobenzaldehyde (C<sub>9</sub>H<sub>11</sub>NO, 99%) were used as starting materials. Mg and B were weighed out as Mg : B = 1.05 : 2, while C<sub>9</sub>H<sub>11</sub>NO was added 0%, 2%, and 4% of total weight, respectively (for 4wt.% doped sample, the C atomic percent in the raw powders is 3.55%). After they were ball-milled in air for an hour, the powders were packed into pure iron tubes with an outer diameter of 8 mm, and an inner diameter of 5 mm. Then the tubes were rotary-swaged and drawn to wires of 1.75 mm in diameter. Subsequently, the wires were rolled to tapes of 3.7 mm in width and 0.5 mm in thickness (fill factor ~29%). The final tapes were cut and wrapped in Ti foil to minimize the oxidation of the samples, then sintered at 700-850°C for an hour in flowing high purity Ar, followed by a furnace cooling to room temperature.

The phase constitution and microstructure of the samples were investigated using X-ray diffraction (XRD) and scanning electron microscope (SEM). Magnetization of the samples was measured by a SQUID magnetometer (Quantum Design, MPMS XL-7). After peeling away the Fe sheath, resistivity curves were measured with an Oxford cryogenic system (Maglab-12), and the  $H_{c2}$  and  $H_{irr}$  were obtained from the 90% and 10% values of the normal-state resistance. The transport current ( $I_c$ ) at 4.2 K and 20 K were evaluated by a standard four-probe technique, with a criterion of 1 μV/cm. Current leads and voltage taps were directly soldered to the sheath material of MgB<sub>2</sub> tapes. A magnetic field was applied parallel to the tape surface.

## 3. Results and discussions

XRD patterns of undoped samples annealed at 800°C and 4% C<sub>9</sub>H<sub>11</sub>NO doped samples sintered at different temperatures were shown in figure 1. As can be seen, the main phase of all these samples is MgB<sub>2</sub>, with small amount of MgO. This is a common phenomenon in MgB<sub>2</sub> samples. Mg is an oxidative element, so the

formation of MgO can not be absolutely excluded during the tape fabrication process. But it was reported that some small size MgO particles can act as pinning centers and enhance the pinning ability of MgB<sub>2</sub> material. Besides MgO, Fe diffraction peak, which came from the sheath material, also appeared. Actually, there was a detectable reaction layer between the Fe sheath and superconducting core for all of the samples. For the samples sintered at 850°C, the reaction layer was about several micrometers in thickness.

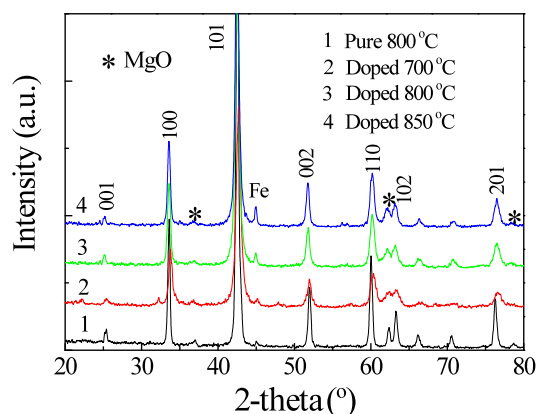


Fig.1 XRD patterns of undoped samples sintered at 800 °C and 4% C<sub>9</sub>H<sub>11</sub>NO doped samples heated at different temperatures. The peaks of MgB<sub>2</sub> indexed, while the peaks of MgO are marked by asterisks.

On the other hand, the in-plane full width at half maximum (FWHM) of the (110) and (100) peaks for the doped tapes are apparently larger than those of the undoped one. This means that the crystallization of the doped samples was degraded due to the C substitution or the impurities introduced by doping. The lattice parameters of undoped samples and 4% doped samples were obtained from the analysis of the diffraction data using the X<sub>pert</sub> program. It was found that the lattice parameter  $a$  was decreased from 3.0829 Å for undoped samples to 3.0771 Å for doped samples sintered at 800°C. But the lattice parameters for doped samples sintered at different temperatures did not have much difference. For example, the lattice parameter  $a$  for doped samples sintered at 700, 800, 850 °C was 3.0784, 3.0771, and

3.0770 Å, respectively. The shrinkage of lattice parameter  $a$  is attributed to the substitution of C for B, which usually happens in  $\text{MgB}_2$  samples doped with carbon containing materials. A distortion of the honeycomb B sheet may result in an improvement of intraband scattering, and thus enhance  $H_{c2}$  through a reduction of coherence length  $\xi$  [6].

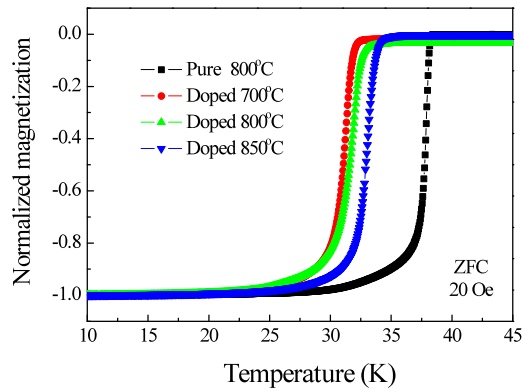


Fig.2 Temperature dependence of the DC magnetic susceptibility curves of undoped samples annealed at 800 °C and 4%  $\text{C}_9\text{H}_{11}\text{NO}$  doped samples sintered at different temperatures.

Superconducting transition of the undoped samples heated at 800°C and doped samples annealed at different temperatures were measured by the DC magnetization method. As shown in figure 2, the onset  $T_c$  of doped samples sintered at 700, 800, 850 °C was 32, 32.9, and 33.8 K, respectively. This is comparable to that of carbon samples heat treated at the same temperature. The linear increase of  $T_c$  with increasing heating temperature can be easily understood, as higher heating temperature brings better crystallization. Meanwhile, it should be noted that the undoped samples show a higher  $T_c$  compared to that of the doped samples sintered at the same temperature.

Figure 3 shows transport  $J_c$  vs. magnetic field curves of the 2% and 4%  $\text{C}_9\text{H}_{11}\text{NO}$  doped samples sintered at different temperatures. The data of undoped samples heated at 800°C are also included for comparison. Only data above 9 T are shown, because at lower field region,  $J_c$  was too high to be measured. Compared to the undoped samples, the in-field  $J_c$

property of  $\text{C}_9\text{H}_{11}\text{NO}$  doped tapes were much improved, indicating an enhanced flux pinning ability. 4% doped samples show higher  $J_c$  than the 2% doped ones at each corresponding temperature, indicating a high doping tolerance of  $\text{C}_9\text{H}_{11}\text{NO}$  in  $\text{MgB}_2$ . The highest  $J_c$  values were obtained in the 4% doped samples annealed under 800°C. For example, at 4.2K, 10T,  $J_c$  reached  $3.7 \times 10^4 \text{ A/cm}^2$ . According to our knowledge, this is the highest  $J_c$  value observed in carbohydrates doped  $\text{MgB}_2$  tapes, only slightly lower than that in  $\text{C}_{60}$  doped samples or ball-milled carbon doped samples.

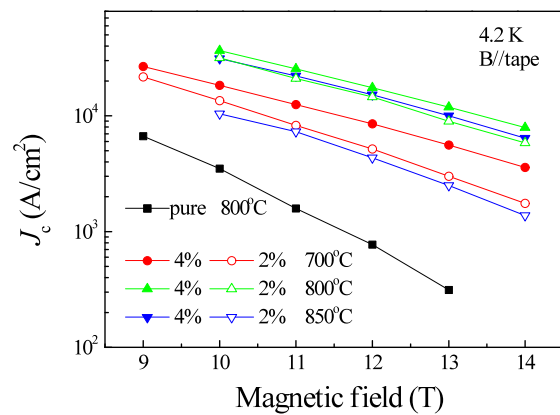


Fig.3 Transport  $J_c$ - $B$  properties of Fe-sheathed undoped and doped tapes. The measurements were performed in magnetic fields parallel to the tapes surface at 4.2 K.

It is found that the electrical resistivity ( $\rho$ ) values at 40 K for pure and  $\text{C}_9\text{H}_{11}\text{NO}$  doped  $\text{MgB}_2$  samples sintered at 800°C were 30.9 and 130  $\mu\Omega\text{-cm}$ , respectively. This indicates that the electrical resistivity  $\rho(40\text{K})$  for doped sample is higher than the undoped samples. At the same time, the residual resistivity ratio  $\text{RRR} = \rho(300\text{K})/\rho(40\text{K})$  was decreased from 1.95 for undoped samples to 1.41 for 4% doped samples sintered at 800°C. The higher  $\rho$  values for the doped sample can be partly explained by the non-superconducting and generally insulating second phases present in the  $\text{C}_9\text{H}_{11}\text{NO}$  doped samples [4]. Another reason is likely attributed to the enhancement in intraband scattering, induced by C substitution.

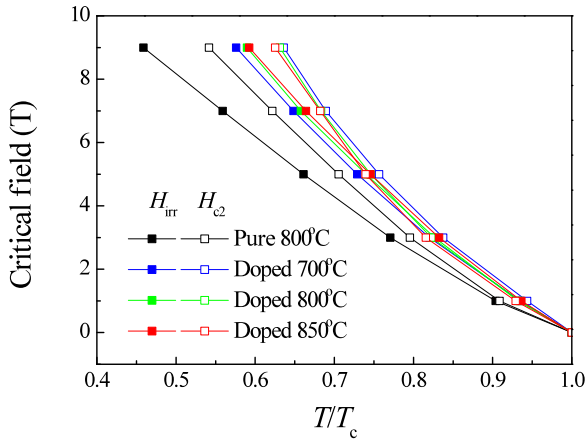


Fig.4  $H_{irr}$  values as a function of the temperature for the different acetone doped level samples heated at 700 °C. Inset: variation of  $H_{c2}$  with temperature.

Normalized temperature dependence of  $H_{c2}$  and  $H_{irr}$  for undoped samples heated at 800°C and  $C_9H_{11}NO$  doped samples sintered at different temperatures was shown in figure 4. Clearly, the  $H_{c2}$  and  $H_{irr}$  of the doped tapes increase more rapidly with decreasing temperature than that of the undoped one. The improved  $H_{c2}$  is originated from a reduced coherence length  $\xi$ , which attributes to the enhanced intraband scattering by C substitution into B sites, as predicted by the theoretical models. This is confirmed by the smaller  $a$ -axis lattice parameter and lower residual resistivity ratio of doped samples than those of pure samples.

Transport measurements at 20 K fields up to 6 T were also conducted for pure and doped tapes annealed at 800°C. It's found that the  $J_c$  values of  $C_9H_{11}NO$  doped samples are clearly higher than those of undoped samples in all the magnetic fields, especially in high field regions. As reported, the critical current density in self-field increases with the improvement of grain connectivity. So the  $J_c$  improvement by  $C_9H_{11}NO$  doping not only results from  $H_{c2}$  enhancement, but also from the melioration of the grain linkages. More importantly, this  $J_c$  behavior of  $C_9H_{11}NO$  doped sample made it likely to be useful in liquid helium free magnetic resonance imaging (MRI) devices, although the  $T_c$  was suppressed a little due to the C substitution.

Doping with carbohydrates is well known to be the most effective way add C element homogeneously into the  $MgB_2$  tapes and wires. The melting point of  $C_9H_{11}NO$  is only about 70°C, meaning that the  $C_9H_{11}NO$  would be in liquid state before chemical reaction happens, making a homogeneously distribution in raw materials. On the other hand,  $C_9H_{11}NO$  decomposes at a temperature below the formation temperature of  $MgB_2$  phase, so it can provide highly reactive C during the formation of  $MgB_2$  phase. The C element released from decomposition can effectively substitute into B sites. And the substitution of C for B induces disorder on the lattice sites, leading to the enhancement of the  $H_{c2}$ . This is thought as the main reason for the superior field dependence of  $J_c$  in the  $C_9H_{11}NO$  doped samples.

#### 4. Conclusion

$C_9H_{11}NO$  doped samples were fabricated using the *in situ* PIT method. XRD analysis indicates that  $a$ -axis of  $MgB_2$  lattice shrank in doped samples. The  $H_{c2}$  and  $H_{irr}$  were obviously enhanced by  $C_9H_{11}NO$  doping.  $J_c$  of 4%  $C_9H_{11}NO$  doped samples heat treated at 800°C reached 37,000A/cm<sup>2</sup> in 10 T, and 11,000A/cm<sup>2</sup> in 13 T at 4.2 K. These  $J_c$  values are much higher than those of other carbohydrates doped  $MgB_2$  tapes, suggesting that there are possibility to fabricate  $MgB_2$  tapes with excellent transport  $J_c$  under high field at 5~20 K using carbohydrate as dopant.

#### References

- [1] J. Nagamatsu, et al., Nature 410, 63 (2001).
- [2] Y. W. Ma, et al., Appl. Phys. Lett. 88, 072502 (2006).
- [3] A. Matsumoto, et al., Appl. Phys. Lett. 89, 132508 (2006).
- [4] Y. Zhu, et al., J. Appl. Phys. 102, 013913 (2007)
- [5] R. Flükiger, et al., Supercond. Sci. Technol. 22, 085002 (2009).
- [6] Z. S. Gao, et al., J. Appl. Phys. 102, 013914 (2007).